

RSC Advances



This is an *Accepted Manuscript*, which has been through the Royal Society of Chemistry peer review process and has been accepted for publication.

Accepted Manuscripts are published online shortly after acceptance, before technical editing, formatting and proof reading. Using this free service, authors can make their results available to the community, in citable form, before we publish the edited article. This *Accepted Manuscript* will be replaced by the edited, formatted and paginated article as soon as this is available.

You can find more information about *Accepted Manuscripts* in the [Information for Authors](#).

Please note that technical editing may introduce minor changes to the text and/or graphics, which may alter content. The journal's standard [Terms & Conditions](#) and the [Ethical guidelines](#) still apply. In no event shall the Royal Society of Chemistry be held responsible for any errors or omissions in this *Accepted Manuscript* or any consequences arising from the use of any information it contains.

Gas-Breathing Polymer Film for Constructing of Switchable Ionic Diodes

Hong Jiang^{†}, Erkang Wang[‡], Jiahai Wang^{†*},*

[†]National Engineering Research Center for Colloidal Materials, Shandong University, Jinan 250100, People's Republic China. [‡]State Key Laboratory of Electroanalytical Chemistry, Changchun Institute of Applied Chemistry, Chinese Academy of Sciences, Changchun, Jilin, 130022, China.

E-mail: jiahai_wang@sdu.edu.cn

Tel: +86-053188363180

[Insert Running title of <72 characters]

1 ABSTRACT

2 Carbon dioxide (CO₂) as one of the major byproduct of cellular metabolism mediates many
3 fundamental behaviors, whose detection is associated with the activation of protein ion channels
4 expressed on the olfactory sensory neurons. Inspired by this biological phenomenon, we
5 developed extraordinary gas-sensitive ion channel, reconfigurable ionic diode and bionic ion
6 pump on the basis of growth of gas-responsive polymer film, which can be rendered hydrophilic
7 with the CO₂ stimulus of and hydrophobic with the N₂ stimulus. In particular, by alternatively
8 purging CO₂/N₂ into the solutions which are placed on both sides of the channel embedded in the
9 polymer membrane, the smart polymer-coated channel can be either closed or opened, which is
10 independent of voltage polarity. Most intriguingly, under the asymmetric stimulation with pH
11 pairs (pH 6.5 | | pH 9.0) or with gas inputs (CO₂ | | N₂) for both sides of the channel, change in
12 voltage polarity can switch the channel between close status and open status, leading to
13 construction of reconfigurable fluidic diode. Furthermore, by combination of gas inputs and
14 voltage polarity, each of both gates of the channel can be individually manipulated, which are
15 very important prerequisites for construction of bionic ion pump that can be operated under
16 physiologically mild conditions. It is envisaged that this new progress in bionic pore/channel
17 field will hold great prospects for the application of this kind of biomimetic device in energy
18 storage, sample filtration and seawater desalinization.

19 **Keywords:** Ionic diode, Gas-responsive polymer brush, Track-etched membrane.

20

21

22

[Insert Running title of <72 characters]

23 INTRODUCTION

24 Carbon dioxide (CO₂) has been widely involved in natural activities. The ecosystem has
25 evolved a comprehensive set of CO₂-responsive pathways to make a balance. CO₂ as one of the
26 major byproduct of cellular metabolism mediates many fundamental behaviors, whose detection
27 is associated with the activation of protein ion channels expressed on the olfactory sensory
28 neurons¹⁻⁹ and transportation through biological gas channel^{10, 11}. It will be intriguing to design
29 artificial gas-responsive ion channel, ionic diode and ion pump by mimicking the gas-responsive
30 pathway existing in the living system. Until now, no artificial gas-responsive ion channel, ionic
31 diode and ion pump on the basis of the thin polymer film supported on track-etched membrane
32 have been constructed, although many biomimetic pore/ionic systems have been built up on the
33 basis of immobilization of organic molecules, polymer, and biomolecules onto the
34 pore/channel¹²⁻²³.

35 In recent years, abiotic devices that mimic the function and structure of biological
36 counterparts are alluring increasing attentions. Among these artificial designs, incessant
37 endeavors have been devoted to imitating ion channels, which mainly comprise engineered
38 protein ion channels²⁴, solid nanopores^{20, 25-27} in ultrathin membrane, asymmetric pores^{28, 29} in
39 polymer membrane and glass nanopores^{30, 31}. Heretofore, many bioinspired ion conducting
40 channels are designed based on artificial nanopore with one gate, which can be switched on and
41 off by various external stimuli such as voltage^{32, 33}, temperature³⁴, light³⁵, ion³⁶, pressure³⁷,
42 ATP^{38, 39} and pH^{40, 41}. More recently, Jiang group invented a biomimetic ion pump based on
43 nanochannel with two gates¹³. In that pioneering study, two different responsive polymer brushes
44 were grafted on each end of the ionic channel and each gate can be switched from on to off or
45 vice versa independently/synchronously by pH stimuli.

[Insert Running title of <72 characters]

46 Among those external stimuli, pH stimulus is very appealing and easily accessible, which has
47 been applied to change the size, surface charge and wettability of the channels. However, many
48 operation cycles that require repeated addition of acids and bases into the solution can degrade
49 the switching capability of artificial ion channel and ion pump due to the salt accumulation in the
50 solution. While substituting gas stimuli for pH has several distinct advantages: (1) Salt
51 accumulation due to repeated addition of various pH solution can be eliminated, which can
52 diminish the performance of biomimetic device; (2) Drastic conditions such strong acid and
53 strong base can be replaced by much more mild operation conditions; (3) The whole system can
54 be easily restored to previous status even after many cycles of operations. Furthermore, another
55 common feature for previous external-stimuli responsive ion channels is that responsive
56 monolayer is grafted inside the channel^{16, 18-20}. When the channel/pore is in close status, the
57 leakage and switching efficiency is highly diameter-dependent. Insufficient growth of responsive
58 polymer leads to the failure and leakage of artificial ion pump, whereas overgrowth of
59 responsive polymers will deteriorate the performance of the channel. It will be more encouraging
60 for scientists to develop more intelligent materials and devices with leakage-free property and
61 high switching efficiency.

62 In this work, we develop an ionic channel device both of whose entrances are covered by
63 gas-breathing polymer film, which possess the properties of artificial ion channel, ion pump and
64 ionic diode. Each gate of this ionic channel can be manipulated individually or synchronously.
65 Purging CO₂ into buffer solution (pH 7) on both sides of the channel membrane can render the
66 polymer films positively charged and hydrophilic, leading to the ion transport through the
67 polymer films and to the “on” status of the channel. Whereas, the polymer films can be switched
68 back to hydrophobic status and the channel is completely shut down when the solutions on both
[Insert Running title of <72 characters]

69 sides of the channel membrane were purged with N_2 or replaced with buffer solutions with $pH \geq 7$.
70 Except synchronous manipulation of both polymer films on both sides of the channel membrane,
71 each gate can also be individually operated by combination of gas (or pH) and voltage inputs,
72 which are very important prerequisites for construction of bionic ion pump. Most interestingly,
73 under the asymmetric stimulation with pH pairs (pH 6.5 | | pH 9.0) or with gas inputs (CO_2 | | N_2),
74 change in voltage polarity can switch the channel between close status and open status, leading
75 to construction of reconfigurable ionic diode. The alternative passing of CO_2/N_2 into the solution
76 can allow each gate of the channel to be operated repeatedly for many cycles, which fully
77 eliminates the salt accumulation and degradation of performance. The second advantage lies in
78 that this approach prevents any leakage and lifts the strict requirement on the size of the channel
79 as well. It is envisaged that this new progress in bionic pore/channel field will hold great
80 prospects for the application of this kind of biomimetic device in energy storage, sample
81 filtration and seawater desalinization.

82

83 **EXPERIMENTAL SECTION**

84 **Fabrication of Channel:** PET (polyethylene terephthalate) membranes (diameter = 3 cm,
85 thickness = 12 μm) that had been irradiated with heavy ions of 2.2 GeV kinetic energy to create
86 single track and multi tracks through the membrane were obtained from GSI, Darmstadt,
87 Germany and referred to as the “tracked” membranes. NaOH, HCOOH, Na_2CO_3 and KCl were
88 purchased from Beijing Chemical Reagent Company (Beijing, China). 2A1 was purchased from
89 Dow Corning. All of the chemicals were at least analytical grade. To obtain conically shaped
90 pore, each side of the PET membrane was treated with UV light (4 mW/cm^2) for one hour,

[Insert Running title of <72 characters]

91 respectively to allow the activation of the polymer foil. Polymer membrane was sandwiched
92 between two half compartments each of which contained etching solution (6 M NaOH) and
93 stopping solution (1 M HCOOH plus surfactant 2A1), respectively and the etching temperature
94 was maintained at 40°C. The whole etching process was controlled by monitoring current
95 through the membrane; one volt potential difference was applied. The current remained zero as
96 long as the pore did not break through the membrane. The current after the breakthrough can be
97 monitored via a picoammeter/voltage source(Keithley 6487, Keithley Instruments, Cleveland,
98 OH), when the desired current was reached, the etching process was stopped by replacing the
99 etching solution with the stopping solution to neutralize the etching solution in the pore. After
100 first step etching, the membranes were thoroughly washed with purified water and dried under
101 nitrogen flow. The membrane after first step etching is immersed into a vial containing 2 M
102 NaOH at 65 for 10 minutes. The diameters of the conically shaped channel are obtained by
103 measuring the corresponding diameters of multi-track membrane etched under the same
104 experimental conditions.

105 **Polymer Film Growth Via Surface-Initiated ATRP:** Nascent membranes after chemical
106 etching were immersed in an aqueous solution containing 1% w branched PEI(MW: 25,000) for
107 8 hours in room temperature, and then the samples are wash with ethanol, followed by Nitrogen
108 flow drying. The surface immobilization of ATRP initiator was adapted from previous published
109 procedures⁴². Briefly, 2-bromopropionyl bromide (10 mM) was coupled via amide linkage to the
110 PEI coated membrane surface in buffered solution (pH 10, 32 mM Na₂CO₃). The reaction
111 mixture that was cooled in the ice bath, and bubbled with N₂ for 30 minutes lasted for 24 h under
112 N₂ protection. Regents for polymer brush growth including H₂O, methanol,
113 2-(Diethylamino)ethyl methacrylate, CuBr and N,N,N',N',N''-pentamethyldiethylenetriamine
[Insert Running title of <72 characters]

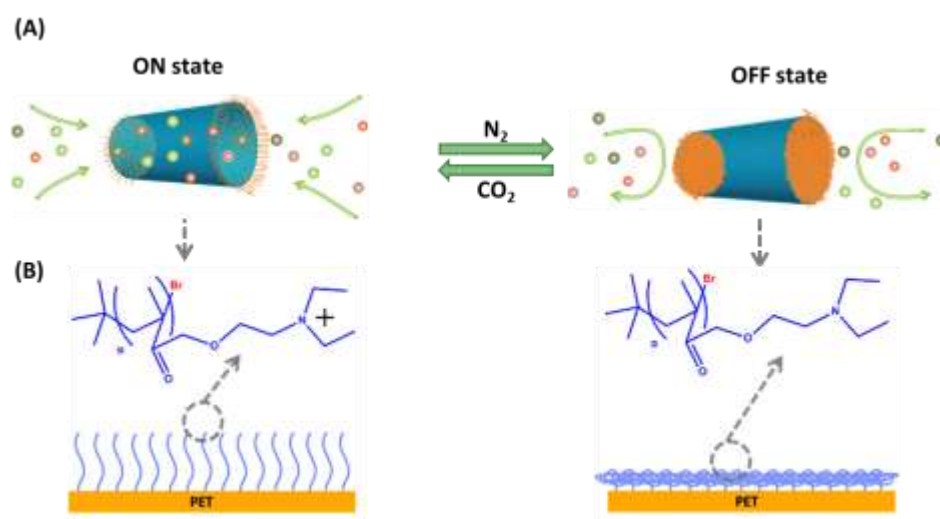
114 (PMDETA) were purchased from JK Chemical (Beijing, China) and used without further
115 purification. The polymerization reaction takes place for 30 minutes under N₂ protection. After
116 the polymerization, the PET film was washed with methanol and dH₂O for several times to
117 remove the redundant CuBr and the other reagents. Then the PET film was dried in the N₂ flow
118 and put in the vacuum for subsequent characterization.

119 **Current-Versus-Voltage Measurements (I-V curve):** The prepared PET film with
120 asymmetrical pore inside was sandwiched between two half components filled with conductive
121 electrolyte in order to measure the I-V curve. The current through the conical-shaped pore was
122 measured with a Keithley 6487 picoammeter (Keithley Instruments, Cleveland, OH) and
123 Ag/AgCl electrodes in a custom-designed electrolyte cell. Transmembrane potentials from -1V
124 to +1V was scanned to obtain each I-V curve. All experiments were carried out in room
125 temperature. Buffered solutions (0.1 M PBS, 0.1M KCl) at pH 3.0, 5.0, 7.0 and 9.0 were used for
126 stimulation. For gas stimulation, buffered solution (0.1 M PBS, 0.1M KCl) at pH 7 after purging
127 of the solution with CO₂/N₂ for desired time was used to open/close the gate, respectively and
128 each gate of the asymmetric pore can be independently operated.

129 RESULTS AND DISCUSSION

130 Endowing the artificial pore with switching features responsive to external stimuli has been
131 the scholastic pursuit in the past several years. Until now, several approaches based on pH^{40,41},
132 metal ion³⁶, voltage^{32,33} and ligand⁴³ have been built up to mediate the open/close status of the
133 pores. In this study, the gas-responsive polymer film has been adopted to cover both entrances of
134 the ionic channel. Figure 1A illustrates the reversible switching process accomplished via
135 alternatively purging CO₂ and N₂ into the buffer solutions close to the track-etched polymer film.
136 In the presence of CO₂, the pH value of the buffer solution drops, leading to the protonation and
[Insert Running title of <72 characters]

137 extension of the polymer and subsequent “on” status of the polymer film (Figure 1B). Purging
138 the buffer solution with N_2 could displace the CO_2 and leads to the increase of pH value, which
139 provokes the deprotonation of polymer film and drives the polymer film toward hydrophobic and
140 collapsed status. The whole modification process is presented in the supporting materials (Figure
141 S1 in supporting information). Additional XPS and NMR characterizations have also proved
142 each modification step (Figure S2 and S3 in supporting information).

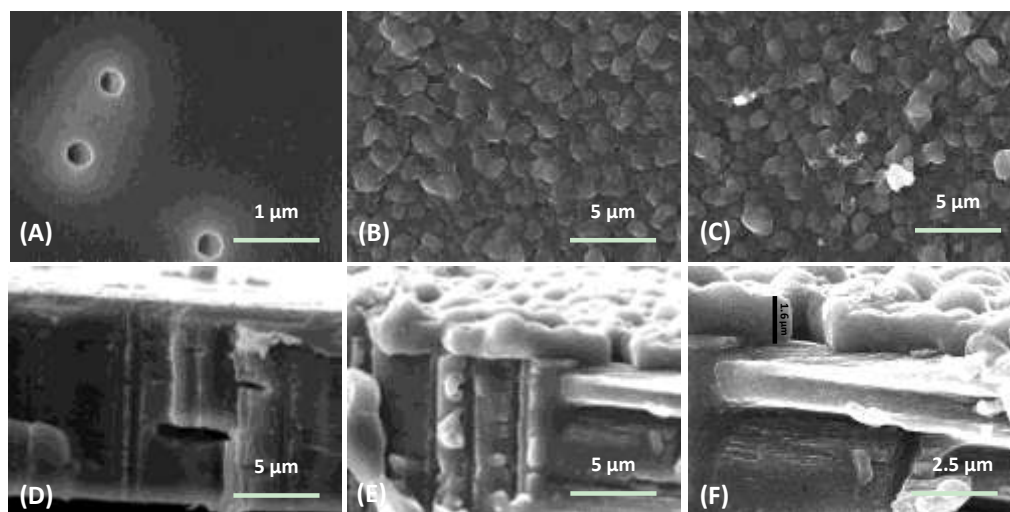


143
144 **Figure 1.** (A) Cartoon illustration of “on” status and “off” status of cylindrical channel covered
145 by polymer films under the symmetric stimulation with gas inputs. (B) charged status due to
146 protonation of polymer film and collapsed status due to deprotonation of the polymer film.

147 To prove the successful growth of gas-responsive polymer film on the channel membrane,
148 SEM images were acquired (Figure 2), including the cross section, the top and bottom sides of
149 the channel. Continuous polymer films fully covered both sides of the channel membrane after 1
150 hour growth (Figure 2B and 2C) and the thickness of the polymer film was measured to be 1.6
151 μm (Figure 2F). It is clear that domains with various sizes exist in the polymer film and have
152 much larger size than the channel diameter (200 nm). From the cross section image (Figure 2E),
153 the polymer film growth majorly happened on the faces of the channel membrane and the inside

[Insert Running title of <72 characters]

154 of the channel was left empty without polymer growth. To the best of our knowledge, growth of
155 gas-responsive polymer film on the channel membrane has not been reported yet.



156
157 **Figure 2.** SEM images of cylindrical channels with diameter of 200 nm before and after polymer
158 film growth. The side view (A) of track-etched membrane (A), the top and bottom views (B and
159 C) of cylindrical channel embedded in PET membrane after polymer film growth; Cross section
160 of the cylindrical channel before (D) and after (E and F) polymer film growth. The thickness is
161 measured to be around 1.6 μm .

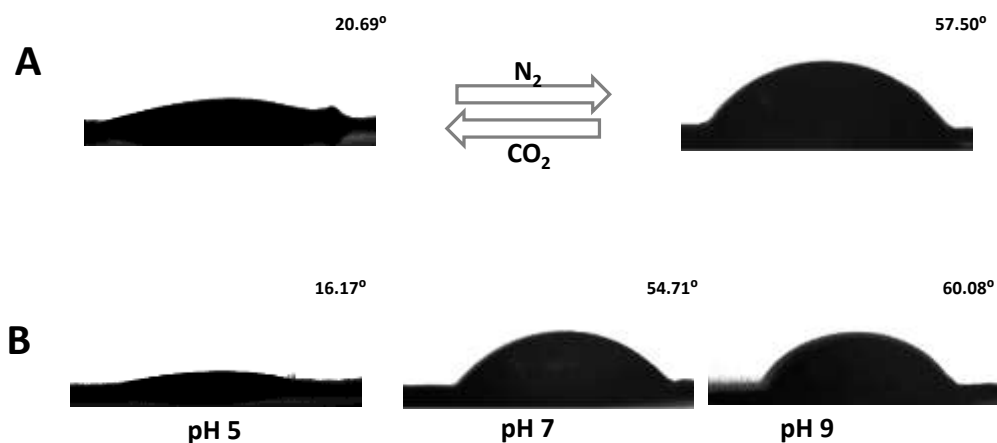
162 Gas-responsive polymer film on the track-etched membrane exhibited repetitive switching
163 between hydrophobicity and hydrophilicity (Figure 3). Contact angle measurements (Figure 3)
164 illustrate that the contact angle of water droplet on the nanopore surface showed contact angle of
165 16.17° after the membrane grafted with polymer film was immersed in pH 5. Whereas after the
166 membrane was immersed in pH 7 buffer and air dried, the contact angle increased to 54.76°
167 (Figure 3B). The contact angle can be further increased if pH 9 solution was used. This result
168 clearly manifested that protonation/deprotonation of the polymer film on the membrane can lead
169 to change in the hydrophilicity/hydrophobicity of the membrane surface. Instead of employment
170 of buffer solutions adjusted with NaOH to certain pH values, buffer solution reversibly purged

[Insert Running title of <72 characters]

171 with CO₂/N₂ can also efficiently switch the membrane status between big contact angel (57.50°)
172 and small contact angle (20.69°) (Figure 3A).

173

174



175

176 **Figure 3.** Contact angle measurements of the polymer film (PDEAEMA: poly
177 2-(Diethylamino)ethyl methacrylate) grafted onto the channel membrane. (A) Measurements
178 were carried out after polymer film was immersed in neutral electrolyte solutions purged with
179 CO₂ and N₂ for 30 minutes, respectively and was nitrogen dried. (B) Measurements were carried
180 out after polymer film was immersed in each electrolyte solution (pH 5, 7 and 9). 0.1 M PBS
181 containing 0.1 M KCl was applied as the electrolyte solution.

182 Previous study¹⁹ proposed that toggling between hydrophobicity and hydrophilicity can
183 play an extremely important role in opening/closure of the channel on the basis of the pH-tuned
184 polymer brush immobilized into the channel. Unambiguously, it has been clarified that
185 conformation variation is a negligible factor which contributes to the ion transport through this
186 kind of channel. In contradiction with immobilization of the polymer brush inside the channel,
187 the present study entails only growth of gas-responsive polymer film on both sides of the
188 track-etched membrane, which can fully prevent leakage of the channel embedded in the
189 membrane once the channel is switched to “off” status. Notably, several previous nanochannels
190 with responsive property are majorly related with conformation switching of the monolayer
[Insert Running title of <72 characters]

191 immobilized inside the nanochannel surface. Obviously, this is not the same as our case. As
192 shown in Figure S4 (supporting information), in the presence of different pH values (5, 7 and 9),
193 the morphology of the polymer film characterized by SEM did not show any distinct difference
194 and the channel membrane was consistently covered by continuous polymer film, which means
195 that the conformation switching is not the important factor contributing to ion transport through
196 the channel. Furthermore, the thickness of the polymer film was up to 1.6 μm , which was several
197 times larger than the diameter of the channel embedded in the PET membrane.

198 Except XPS and NMR characterization of polymer film growth, each step in the
199 modification process was confirmed and characterized with current-versus-voltage curve (I-V
200 curve). In this study, we presented I-V curves for one cylindrical channel with diameter of 200
201 nm and another conical-shaped channel with tip diameter of 130 nm. The cylindrical channel in
202 the PET membrane was fabricated under the same conditions as those in Figure 2. The I-V curve
203 (black curve in Figure 4A) of the single cylindrical channel without any modification showed
204 linear shape without any rectification, which is measured in 100 mM PBS solution containing
205 1M KCl at pH 3. Further tandem modification with branched PEI and initiator not exhibited
206 much difference in the current-versus-voltage curves. As compared to cylindrical channel,
207 asymmetric channel after PEI adsorption (red curve, Figure 4C) presented upward curve with
208 strong rectification. For both cylindrical and asymmetric channel, the polymer film growth fully
209 blocked ion transport through the channel when being measured in 0.1 M KCl with pH 7 solution
210 (curves in dark cyan, Figure 4A and C).

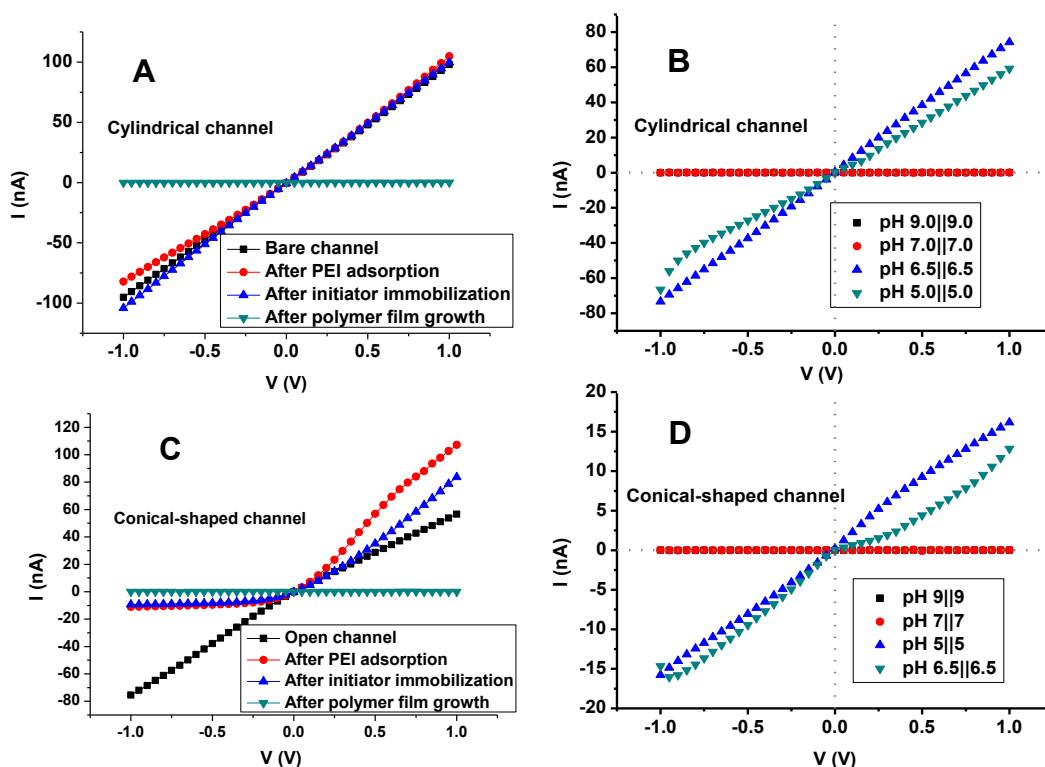
211

212

213

[Insert Running title of <72 characters]

214
215
216
217
218
219
220
221
222
223
224
225



226 **Figure 4.** (A) I-V characterization of each modification step for the cylindrical channel with
 227 diameter of 200 nm. (B) pH-dependent switching between “on” status and “off” status of the
 228 cylindrical channel covered by polymer film. (C) I-V characterization of each modification step
 229 for conical-shaped channel with tip diameter of 130 nm and base diameter of 957 nm. (D)
 230 pH-dependent switching between “on” status and “off” status of the conical-shaped channel
 231 covered by polymer film. Electrolyte solution for experimental measurements in (A) and (C) is
 232 0.1 M PBS containing 1 M KCl at pH 3; Buffer solution for experimental measurements in (B)
 233 and (D) is 0.1 M PBS containing 0.1 M KCl at pH 7.

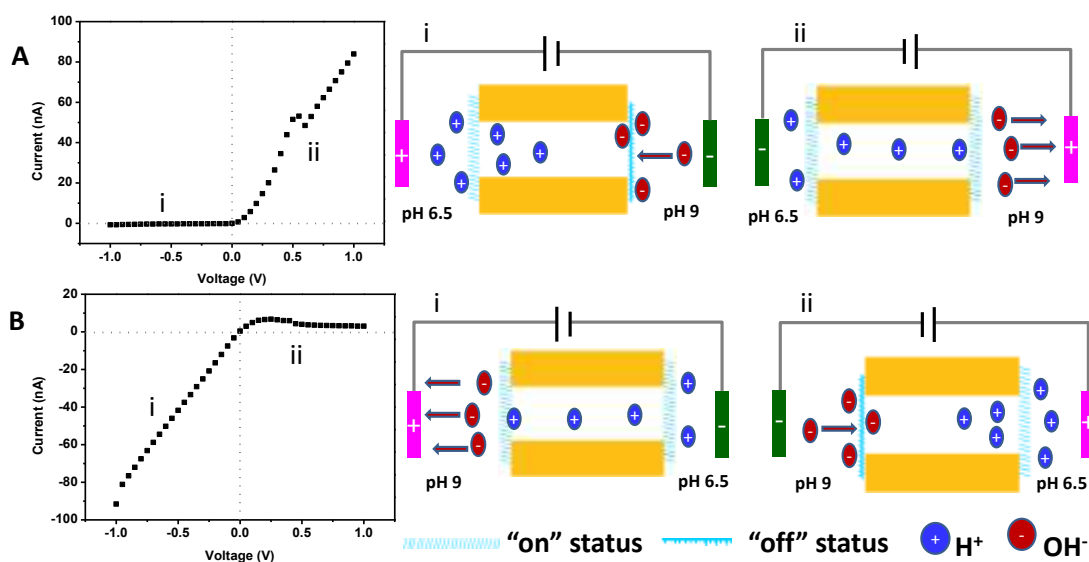
234 Both cylindrical and asymmetric channel covered with gas-responsive polymer film can be
 235 switched on/off by the pH stimuli or gas inputs (Figure 4B and 4D). Ion channel behaviors
 236 common to biological nanopore can be faithfully reproduced: when the pH value is above 7, the
 237 channel can be fully blocked with symmetric pH 7||7 and 9||9 conditions; when pH value is
 238 decreased towards 6.5, the channel can be restored to “on” status with symmetric pH 6.5||6.5
 239 and pH 5||5 conditions. If the on/off current ratio was defined as the ratio of the current

[Insert Running title of <72 characters]

240 measured at pH 6.5/6.5 to the current measured at pH 9/9, the on/off current ratio corresponding
241 to 1 V was calculated to be 34418 for the cylindrical channel with diameter of 200 nm.
242 Furthermore, the current corresponding to the “off” status measured at 1V was only 2.1 pA,
243 which was defined as the leaking current. To the best of our knowledge, these were the biggest
244 on/off current ratio and the lowest leakage current. As for asymmetric channel with tip diameter
245 of 130 nm and base diameter of 957 nm, the on/off current ratio and the leaking current were
246 6736 and 1.9 pA, respectively, which is calculated from data in Figure 4D. This is to say, the
247 geometry of the channel was not critical factor for determining the switching efficiency. The
248 quality of gas-responsive polymer film itself could play a crucial rule. The pH-adjusted ion
249 transport through the channel both sides of which were covered with gas-responsive polymer
250 film was highly consistent with the pH-dependent switching between hydrophobicity and
251 hydrophilicity.

252 Features belong to ionic diode can be exactly reproduced by this channel system
253 symmetrically functionalized with the same gas-responsive polymer films. It has to be noted that
254 previous ionic diodes based on channel were almost accomplished via asymmetric
255 functionalization with differently charged ligands or polymer brushes^{13, 14, 16, 44, 45}. In the current
256 study, symmetric growth of the same gas-responsive films was executed on both sides of the
257 channel. As shown in Figure 5A, the upward curve with nonlinear shape was divided into two
258 parts including part I and part II. The corresponding cartoons about the ion transportation were
259 also illustrated on the right side. When the buffer solution at pH 6.5 was placed on the left side of
260 the channel and another same solution at pH 9 was placed on the right side of the channel, the
261 voltage polarity decided the status of the channel. When positive voltage was applied on the right
262 side of the channel (part II in Figure 5A), the slope of the I-V curve corresponded to “on” status ,
[Insert Running title of <72 characters]

263 which was exactly same as the case when both sides of the channel were placed with buffer
 264 solutions at pH 6.5 (Figure 4B). When negative voltage was applied (part I), the channel was
 265 completely shut down. The “on” status and “off” status of the channel was exchangeable by
 266 swapping the position of the buffer solutions as shown in Figure 5B.



267
 268 **Figure 5.** Switchable ionic diode pair (A and B) based on the same cylindrical channel covered
 269 by gas-responsive polymer films. Each curve is divided into part I and part II. The corresponding
 270 cartoons illustrate the ion transport mechanisms under pH stimulation and voltage polarity.
 271 When the OH⁻ ions accumulate around the polymer film, this gate is shut down due to
 272 deprotonation and hydrophobicity; when the OH⁻ ions decrease and H⁺ ions dominate around the
 273 polymer film, the gate open up due to protonation and hydrophilicity.

274 Why did voltage polarity play such a significant impact on the ion transport through the
 275 channel when the channel covered by two same polymer films was stimulated under asymmetric
 276 pH conditions? To better understand this phenomenon, we have to understand the movement of
 277 ions under the applied voltage. When negative voltage (Part I in Figure 5A) was applied in
 278 chamber containing the buffer solution at pH 9, the negative ion such as OH⁻ in the same
 279 chamber moved towards the polymer films and the concentration of OH⁻ around the film
 280 increased, leading to closure of the polymer film due to deprotonation and hydrophobicity. When
 [Insert Running title of <72 characters]

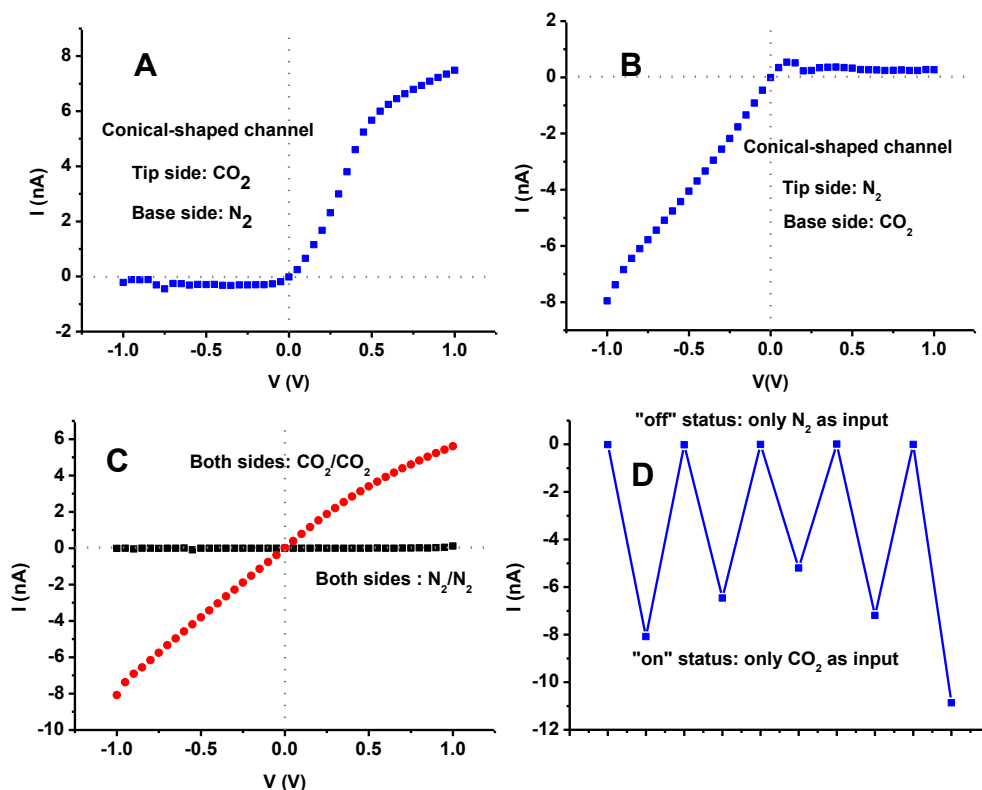
281 positive voltage (Part II in Figure 5B) was applied in chamber containing the buffer solution at
282 pH 9, the negative ion such as OH^- in the same chamber moved away from the polymer films
283 and the concentration of OH^- around the film decreased. Although the H^+ ion in another chamber
284 containing electrolyte solution at pH 6.5 moved away from the polymer film adjacent to the
285 chamber which contained the electrode applying positive voltage, its concentration still
286 overwhelms that of OH^- , leading to the “on” status of the polymer film due to protonation of the
287 polymer film and hydrophilicity. This similar mechanism can be also applied to explain the
288 download curve observed in Figure 5B. Now, it is also very clear that by combining stimuli such
289 as pH and gas with voltage polarity, each one of the two gates can be selectively shut down or
290 open up, which is the important prerequisite for construction of ion pump with alternative gates
291 and occluded states.

292

293

294

[Insert Running title of <72 characters]



295

296 **Figure 6.** Green gas (CO_2 and N_2) breathing ionic diode (A and B) and ion channel (C). In case
 297 (A), the electrolyte solution in the tip side of the conical-shaped channel was purged with CO_2
 298 for 20 minutes and the base side electrolyte solution was purged with N_2 for 20 minutes. In case
 299 (B), the electrolyte solution in the tip side of the conical-shaped channel was purged with N_2 for
 300 20 minutes and the electrolyte solution in the base side was purged with CO_2 for 20 minutes. In
 301 case (C), electrolyte solutions in both sides were purged with CO_2 or N_2 . (D) Repetitive
 302 switching between “on” status and “off” status upon alternative purging with CO_2 and N_2 : each
 303 point value was measured by applying -1 V voltage.

304 Once again, features of this type of diode device which can be explained by the above
 305 mechanism can also be realized by asymmetric channel covered by the two same polymer films
 306 (Figure S5 and S6, Supporting Information). Most interestingly, this kind of ionic device is not
 307 only pH-actuatable but also highly CO_2/N_2 -stimulable. By utilization of asymmetric channel as a
 308 gas-responsive prototype, we carried out a series of experiments to challenging this kind of
 309 channel device with gas stimuli. Upon purging CO_2 into the buffer solution (0.1 M PBS, pH 7,
 310 0.1 M KCl), the pH value changed towards 5; with passing N_2 into the solution, the pH value of

[Insert Running title of <72 characters]

311 7 was recovered. Once the tip and base side solutions of the conical-shaped channel were purged
312 with CO₂ and N₂, respectively, the I-V curve demonstrated extreme high rectification behavior
313 and unprecedented on/off current ratio with upward nonlinear shape (Figure 6A). One unique
314 feature for this channel device is that the current rectification can be fully inverted. Upon
315 purging N₂ and CO₂ into the tip and base side solutions of the same device, the downward I-V
316 curve with excellent high rectification and on/off current ratio was obtained (Figure 6B). The
317 rectification inversion and current direction were highly reversible, which was only dependent on
318 the gas pair (CO₂ || N₂ or N₂ || CO₂). Additionally, as shown in Figure 6C and 6D, more than 5
319 times switching cycles between “on” status and “off” status have been presented in this study
320 under the alternative stimulation with symmetric gas pair (N₂ || N₂ and CO₂ || CO₂).

321 In this paragraph, we would like to clarify that under the unsymmetrical stimulation, the
322 competition between H⁺ and OH⁻ plays a dominant role in the status of the polymer film. By
323 using conical-shaped channel as prototype, we compared three different pH pairs (pH 5 || 7, pH
324 6.5 || 7, and pH 6.5 || 9). As shown in Figure S7, only pH 6.5 || 9 among three pH pairs offered
325 the opportunity to observe the ionic diode behavior: the “on” and “off” statuses are determined
326 by voltage polarity. Figure S7A and S7B conclusively affirmed that H⁺ won and only “on” status
327 was present, which was indicated by the curve shape of the I-V curve. Therefore, the
328 combination of voltage polarity and the appropriate pH pair is crucial for opening and closure of
329 each polymer film gate.

330

331 CONCLUSIONS

[Insert Running title of <72 characters]

332 In summary, we describe a new ionic diode with both entrances covered by the same
333 gas-responsive polymer films. Under the symmetric stimulation with pH pairs (5 || 5, 6.5 || 6.5,
334 7 || 7 and 9 || 9) or with gas pairs (CO₂ || CO₂ and N₂ || N₂), features common to ion channel can
335 be faithfully reproduced including “on” status and “off” status. Under the asymmetric
336 stimulation with gas pairs (CO₂ || N₂, N₂ || CO₂), ionic diode based on gas-responsive polymer
337 films supported on channel membrane can be constructed with the unprecedentedly high
338 rectification ratio more than several thousands and the smallest leaking current around several
339 pA. Most importantly, the diameter and geometry of channel are no longer the critical
340 determining factors that influence the switching efficiency and contribute to current leakage,
341 whereas the quality of the ionic device is more reliant on the polymer films. Except construction
342 of artificial ion channel and ionic diode, this new device can also be applied to build ion pump
343 since both gates of this device can be individually manipulated by combination of gas pairs (or
344 pH pairs) and voltage polarity. Therefore, this device developed herein holds great promise in
345 further applications such as energy field, sample filtration and seawater desalination.

346

347 **ACKNOWLEDGMENT**

348 This work was supported by National Natural Science Foundation of China (No. 21275137
349 and 21190040) and supported by the Fundamental Research Funds of Shandong University
350 (2015TB005)

351

352

353

[Insert Running title of <72 characters]

354

355 REFERENCES

- 356 1. Sun, L.; Wang, H.; Hu, J.; Han, J.; Matsunami, H.; Luo, M. Guanylyl cyclase-D in the
357 olfactory CO₂ neurons is activated by bicarbonate. *Proc. Natl. Acad. Sci. U. S. A.* 2009, 106,
358 2041-2046.
- 359 2. Wang, X.; Zhong, M.; Liu, Q.; Aly, S. M.; Wu, C.; Wen, J. Molecular characterization of the
360 carbon dioxide receptor in the oriental latrine fly, *Chrysomya megacephala* (Diptera:
361 Calliphoridae). *Parasitol. Res.* 2013, 112, 2763-2771.
- 362 3. Su, J.; Yang, L.; Zhang, X.; Rojas, A.; Shi, Y.; Jiang, C. High CO₂ chemosensitivity versus
363 wide sensing spectrum: a paradoxical problem and its solutions in cultured brainstem neurons. *J.*
364 *Physiol.* 2007, 578, 831-841.
- 365 4. Sharabi, K.; Charar, C.; Friedman, N.; Mizrahi, I.; Zaslaver, A.; Sznajder, J. I.; Gruenbaum,
366 Y. The Response to High CO₂ Levels Requires the Neuropeptide Secretion Component HID-1 to
367 Promote Pumping Inhibition. *PLoS Genet.* 2014, 10.
- 368 5. Lahiri, S.; Forster, R. E. CO₂/H⁺ sensing: peripheral and central chemoreception. *Int. J.*
369 *Biochem. Cell Biol.* 2003, 35, 1413-1435.
- 370 6. Kwon, J. Y.; Dahanukar, A.; Weiss, L. A.; Carlson, J. R. The molecular basis of CO₂
371 reception in *Drosophila*. *Proc. Natl. Acad. Sci. U. S. A.* 2007, 104, 3574-3578.
- 372 7. Jones, W. D.; Cayirlioglu, P.; Kadow, I. G.; Vosshall, L. B. Two chemosensory receptors
373 together mediate carbon dioxide detection in *Drosophila*. *Nature* 2007, 445, 86-90.
- 374 8. Badsha, F.; Kain, P.; Prabhakar, S.; Sundaram, S.; Padinjat, R.; Rodrigues, V.; Hasan, G.
375 Mutants in *Drosophila* TRPC Channels Reduce Olfactory Sensitivity to Carbon Dioxide. *PLoS*
376 *One* 2012, 7.
- 377 9. Arioli, S.; Roncada, P.; Salzano, A. M.; Deriu, F.; Corona, S.; Guglielmetti, S.; Bonizzi, L.;
378 Scaloni, A.; Mora, D. The relevance of carbon dioxide metabolism in *Streptococcus*
379 *thermophilus*. *Microbiol.-Sgm* 2009, 155, 1953-1965.
- 380 10. Geyer, R. R.; Musa-Aziz, R.; Qin, X.; Boron, W. F. Relative CO₂/NH₃ selectivities of
381 mammalian aquaporins 0-9. *Am. J. Physiol.-Cell Physiol.* 2013, 304, C985-C994.
- 382 11. Geyer, R. R.; Musa-Aziz, R.; Enkavi, G.; Mahinthichaichan, P.; Tajkhorshid, E.; Boron, W.
383 F. Movement of NH₃ through the human urea transporter B: a new gas channel. *Am. J.*
384 *Physiol.-Renal Physiol.* 2013, 304, F1447-F1457.
- 385 12. Quoc Hung, N.; Ali, M.; Neumann, R.; Ensinger, W. Saccharide/glycoprotein recognition
386 inside synthetic ion channels modified with boronic acid. *Sens. Actuators B* 2012, 162, 216-222.
- 387 13. Zhang, H.; Hou, X.; Zeng, L.; Yang, F.; Li, L.; Yan, D.; Tian, Y.; Jiang, L. Bioinspired
388 Artificial Single Ion Pump. *J. Am. Chem. Soc.* 2013, 135, 16102-16110.
- 389 14. Guo, W.; Tian, Y.; Jiang, L. Asymmetric Ion Transport through Ion-Channel-Mimetic
390 Solid-State Nanopores. *Acc. Chem. Res.* 2013, 46, 2834-2846.
- 391 15. Meng, Z.; Bao, H.; Wang, J.; Jiang, C.; Zhang, M.; Zhai, J.; Jiang, L. Artificial Ion Channels
392 Regulating Light-Induced Ionic Currents in Photoelectrical Conversion Systems. *Adv. Mater.*
393 2014, 26, 2329-2334.
- 394 16. Hou, X.; Guo, W.; Jiang, L. Biomimetic smart nanopores and nanochannels. *Chem. Soc. Rev.*
395 2011, 40, 2385-2401.

[Insert Running title of <72 characters]

- 396 17. Mubarak Ali, B. S., Reinhard Neumann, Wolfgang Ensinger. Biosensing with
397 Functionalized Single Asymmetric Polymer Nanochannels. *Macromol. Biosci.* 2009, NA.
- 398 18. Mubarak Ali, S. N., Patricio Ramirez, Ishtiaq Ahmed, Quoc Hung Nguyen, Ljiljana Fruk, S.
399 M., and Wolfgang Ensinger. Optical Gating of Photosensitive Synthetic Ion Channels. *Adv. Funct.*
400 *Mater.* 2012, 22, 390-396.
- 401 19. Yameen, B.; Ali, M.; Neumann, R.; Ensinger, W.; Knoll, W.; Azzaroni, O. Synthetic
402 Proton-Gated Ion Channels via Single Solid-State Nanochannels Modified with Responsive
403 Polymer Brushes. *Nano Lett.* 2009, 9, 2788-2793.
- 404 20. Ruoshan, W.; Gatterdam, V.; Wieneke, R.; Tampe, R.; Rant, U. Stochastic sensing of
405 proteins with receptor-modified solid-state nanopores. *Nat. Nanotechnol.* 2012, 7, 257-263.
- 406 21. Han, C.; Su, H.; Sun, Z.; Wen, L.; Tian, D.; Xu, K.; Hu, J.; Wang, A.; Li, H.; Jiang, L.
407 Biomimetic Ion Nanochannels as a Highly Selective Sequential Sensor for Zinc Ions Followed
408 by Phosphate Anions. *Chemistry-a European Journal* 2013, 19, 9388-9395.
- 409 22. Yameen, B.; Ali, M.; Alvarez, M.; Neumann, R.; Ensinger, W.; Knoll, W.; Azzaroni, O. A
410 facile route for the preparation of azide-terminated polymers. "Clicking" polyelectrolyte brushes
411 on planar surfaces and nanochannels. *Polymer Chemistry* 2010, 1, 183-192.
- 412 23. Ali, M.; Nasir, S.; Quoc Hung, N.; Sahoo, J. K.; Tahir, M. N.; Tremel, W.; Ensinger, W.
413 Metal Ion Affinity-based Biomolecular Recognition and Conjugation inside Synthetic Polymer
414 Nanopores Modified with Iron-Terpyridine Complexes. *J. Am. Chem. Soc.* 2011, 133,
415 17307-17314.
- 416 24. Reiner, J. E.; Balijepalli, A.; Robertson, J. W. F.; Campbell, J.; Suehle, J.; Kasianowicz, J. J.
417 Disease Detection and Management via Single Nanopore-Based Sensors. *Chem. Rev.* 2012, 112,
418 6431-6451.
- 419 25. Puster, M.; Rodriguez-Manzo, J. A.; Balan, A.; Drndic, M. Toward Sensitive Graphene
420 Nanoribbon-Nanopore Devices by Preventing Electron Beam-Induced Damage. *ACS Nano* 2013,
421 7, 11283-11289.
- 422 26. Liu, S.; Lu, B.; Zhao, Q.; Li, J.; Gao, T.; Chen, Y.; Zhang, Y.; Liu, Z.; Fan, Z.; Yang, F.;
423 You, L.; Yu, D. Boron Nitride Nanopores: Highly Sensitive DNA Single-Molecule Detectors.
424 *Adv. Mater.* 2013, 25, 4549-4554.
- 425 27. Guo, Z.; Wang, J.; Hu, Y.; Wang, E. Application of Biomimetic Nanopore Fabricated in
426 Self-Supported Membrane in Analytical Chemistry. *Prog. Chem.* 2011, 23, 2103-2112.
- 427 28. Mara, A.; Siwy, Z.; Trautmann, C.; Wan, J.; Kamme, F. An Asymmetric Polymer Nanopore
428 for Single Molecule Detection. *Nano Lett.* 2004, 4, 497-501.
- 429 29. Siwy, Z.; Heins, E.; Harrell, C. C.; Kohli, P.; Martin, C. R. Conical-Nanotube Ion-Current
430 Rectifiers: The Role of Surface Charge. *J. Am. Chem. Soc.* 2004, 126, 10850-10851.
- 431 30. Vilozny, B.; Actis, P.; Seger, R. A.; Vallmajó-Martin, Q.; Pourmand, N. Reversible Cation
432 Response with a Protein-Modified Nanopipette. *Anal. Chem.* 2011, 83, 6121-6126.
- 433 31. Ding, S.; Gao, C.; Gu, L.-Q. Capturing Single Molecules of Immunoglobulin and Ricin with
434 an Aptamer-Encoded Glass Nanopore. *Anal. Chem.* 2009, 81, 6649-6655.
- 435 32. Powell, M. R.; Cleary, L.; Davenport, M.; Shea, K. J.; Siwy, Z. S. Electric-field-induced
436 wetting and dewetting in single hydrophobic nanopores. *Nat. Nanotechnol.* 2011, 6, 798-802.
- 437 33. Buchsbaum, S. F.; Gael, N.; Howorka, S.; Siwy, Z. S. DNA-Modified Polymer Pores Allow
438 pH- and Voltage-Gated Control of Channel Flux. *J. Am. Chem. Soc.* 2014, 136, 9902-9905.

[Insert Running title of <72 characters]

- 439 34. Zhang, L.-X.; Cai, S.-L.; Zheng, Y.-B.; Cao, X.-H.; Li, Y.-Q. Smart Homopolymer
440 Modification to Single Glass Conical Nanopore Channels: Dual-Stimuli-Actuated Highly
441 Efficient Ion Gating. *Adv. Funct. Mater.* 2011, 21, 2103-2107.
- 442 35. Wang, G.; Bohaty, A. K.; Zharov, I.; White, H. S. Photon gated transport at the glass
443 nanopore electrode. *J. Am. Chem. Soc.* 2006, 128, 13553-13558.
- 444 36. Hou, X.; Guo, W.; Xia, F.; Nie, F.-Q.; Dong, H.; Tian, Y.; Wen, L.; Wang, L.; Cao, L.;
445 Yang, Y.; Xue, J.; Song, Y.; Wang, Y.; Liu, D.; Jiang, L. A Biomimetic Potassium Responsive
446 Nanochannel: G-Quadruplex DNA Conformational Switching in a Synthetic Nanopore. *J. Am.*
447 *Chem. Soc.* 2009, 131, 7800-7805.
- 448 37. Lan, W.-J.; Holden, D. A.; White, H. S. Pressure-Dependent Ion Current Rectification in
449 Conical-Shaped Glass Nanopores. *J. Am. Chem. Soc.* 2011, 133, 13300-13303.
- 450 38. Liu, N.; Jiang, Y.; Zhou, Y.; Xia, F.; Guo, W.; Jiang, L. Two-Way Nanopore Sensing of
451 Sequence-Specific Oligonucleotides and Small-Molecule Targets in Complex Matrices Using
452 Integrated DNA Supersandwich Structures. *Angew. Chem., Int. Ed. Engl.* 2013, 52, 2007-2011.
- 453 39. Jiang, Y.; Liu, N.; Guo, W.; Xia, F.; Jiang, L. Highly-Efficient Gating of Solid-State
454 Nanochannels by DNA Supersandwich Structure Containing ATP Aptamers: A Nanofluidic
455 IMPLICATION Logic Device. *J. Am. Chem. Soc.* 2012, 134, 15395-15401.
- 456 40. Cheng-Yong, L.; Feng-Xiang, M.; Zeng-Qiang, W.; Hong-Li, G.; Wen-Ting, S.; Kang, W.;
457 Xing-Hua, X. Solution-pH-modulated rectification of ionic current in highly ordered
458 nanochannel arrays patterned with chemical functional groups at designed positions. *Adv. Funct.*
459 *Mater.* 2013, 23, 3836-44.
- 460 41. Xia, F.; Guo, W.; Mao, Y.; Hou, X.; Xue, J.; Xia, H.; Wang, L.; Song, Y.; Ji, H.; Qi, O.;
461 Wang, Y.; Jiang, L. Gating of single synthetic nanopores by proton-driven DNA molecular
462 motors. *J. Am. Chem. Soc.* 2008, 130, 8345-8350.
- 463 42. Kumar, S.; Tong, X.; Dory, Y. L.; Lepage, M.; Zhao, Y. A CO₂-switchable polymer brush
464 for reversible capture and release of proteins. *Chem. Commun.* 2013, 49, 90-92.
- 465 43. Sa, N.; Baker, L. A. Rectification of Nanopores at Surfaces. *J. Am. Chem. Soc.* 2011, 133,
466 10398-10401.
- 467 44. Kalman, E. B.; Sudre, O.; Vlassiuk, I.; Siwy, Z. S. Control of ionic transport through gated
468 single conical nanopores. *Anal. Bioanal. Chem.* 2009, 394, 413-419.
- 469 45. Nguyen, G.; Vlassiuk, I.; Siwy, Z. S. Comparison of bipolar and unipolar ionic diodes.
470 *Nanotechnology* 2010, 21, 265301.

471

472

473

474

475

476

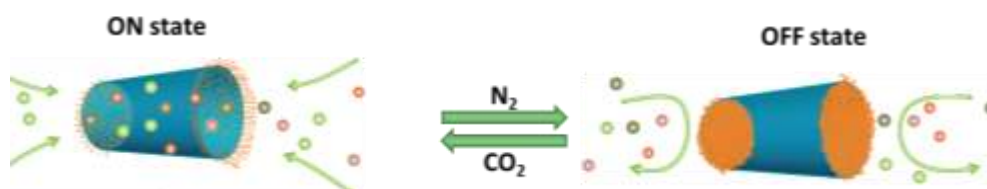
477

[Insert Running title of <72 characters]

478

479 **TOC**

480 We describe a new fluidic channel with both entrances covered by the same gas-responsive
481 polymer films. Under the symmetric stimulation with pH pairs (5 || 5, 6.5 || 6.5, 7 || 7 and 9 || 9)
482 or with gas pairs (CO_2 || CO_2 and N_2 || N_2), features common to ion channel can be faithfully
483 reproduced including “on” status and “off” status. Under the asymmetric stimulation with gas
484 pairs (CO_2 || N_2 , N_2 || CO_2), fluidic diode based on gas-responsive polymer films supported on
485 channel membrane can be constructed with the unprecedentedly high rectification ratio



486

487

488

489

[Insert Running title of <72 characters]